Positioning of Radio Emission Sources with Unmanned Aerial Vehicles using TDOA-AOA Measurement Processing

G.A. Fokin[1]

[1]The Bonch-Bruevich Saint-Petersburg State University of Telecommunications, Prospekt Bolshevikov 22-1, Saint-Petersburg, Russia, 193232

Abstract. Actual trends in current passive geolocation system development includes cooperation of flying segment based on receiver stations aboard Unmanned Aerial Vehicles (UAVs) with terrestrial segment including stationary ground receiver stations. Existing accuracy results achieves the order of tens and hundreds of meters in optimistic Line of Sight (LOS) conditions. However, the problem of radio emission sources positioning with UAVs is especially relevant for search and rescue operations in heterogeneous terrain, when separate primary measurements obtained, for example, after reflections, could lead to a significant error. One possible way to improve the accuracy of positioning in such conditions is to use aerial passive geolocation based on UAVs with joint processing of Time Difference of Arrival (TDOA) and Angle of Arrival (AOA) primary measurements. The contribution of the current investigation is the development of mathematical model for positioning of radio emission sources with UAVs using TDOA-AOA measurement processing.

1. Introduction

Actual trends in current wireless networks development includes joint cooperation of flying segment based on transceiver stations aboard Unmanned Aerial Vehicles (UAVs) with terrestrial segment including stationary ground transceiver stations [1]. Location-based services in such networks could include both military applications, for example, in tactical wireless networks [2] or battlefield environments [3] and civil applications, for example, in ground-aerial surveillance [4], cognitive radio communications [5], [34] or supporting search and rescue operations [6].

Passive geolocation is treated as position estimation of a stationary or mobile transmitter or radiating emitter from passive primary measurements of the arrival times, directions of arrival, or Doppler shifts of electromagnetic waves received at various sites [7]. In the context under consideration various sites are represented by ground and uav based receiver stations.

UAV based passive geolocation techniques had already got considerable attention in the past years and can be subdivided by primary measurements into Time Difference of Arrival (TDOA) [8]–[10], Frequency Difference of Arrival (FDOA) [11], Angle of Arrival (AOA) [12]–[14] and Received Signal Strength Indication (RSSI) [15]–[17] positioning.

Every measurement processing technique based on TDOA, FDOA, AOA or RSSI has its advantages and shortcomings for a specific UAV based geolocation application scenario. While TDOA and FDOA measurement processing technique could achieve high location accuracy in optimistic Line of Sight (LOS) conditions, it requires precise sensors synchronization. If positioning is carried out by TDOA in three-dimensional space, at least four stationary receiving sensors are required. On the other hand, DOA measurement processing technique requires less number of receiving sensors and neither

synchronization among them, however it needs an antenna array for each sensor and resulting location accuracy is highly dependent on the distance between the object of location and sensors. RSSI based localization is preferred in many applications including UAV based localization because of the simplicity in hardware and implementation, however its location accuracy degrades in large scale environments due to inherent variation of characteristics of the received signal strength (RSS).

To reduce the number of sensors required by TDOA processing technique, [8] proposed the use of UAVs as moving sensor platforms in conjunction with ship/land-based platforms to obtain multiple time difference of arrival measurements. Recursive location estimation of a stationary and moving emitter from a pair of unmanned aerial vehicles, using time difference of arrival measurements, formed by the correlation of signals received by two UAVs, is investigated for Kalman [9] and Gaussian [10] filtering techniques. Mobile emitter geolocation and tracking using TDOA and FDOA measurement fusion is considered in [11].

Hierarchical DOA estimation and the fusion of DOAs and the terrain map is proposed in [12] to reduce computational complexity of the near-real-time detection in unmanned airborne emitter monitoring system. A novel application of a common RF direction-finding technique called pseudo-Doppler using small, unmanned system is investigated in [13]. In [14] a series of both real-world flight testing and computer simulated scenarios were conducted to study the feasibility of a low-cost UAV DOA geolocation platform.

RSSI localization and tracking architecture, where a data driven neural network model is used for estimating the unknown signal strength and extended Kalman filters are utilized for eliminating the RSS noise is presented in [15]. Work [16] investigates the impact of UAVs, equipped with RSSI sensors, formation and trajectory on the aerial RF source localization performance for Differential Received Signal Strength Indication (DRSSI) based approach in None LOS (NLOS) propagation conditions. Localization of a radio frequency (RF) transmitter with intermittent transmissions as quickly as possible via a group of UAVs equipped with omnidirectional RSS sensors is considered in [17].

Existing accuracy results in local positioning systems using UAVs achieves the order of tens and hundreds of meters in optimistic LOS conditions and is far from high precision satellite navigation systems [32-33].

However, the problem of radio emission sources positioning with UAVs is especially relevant for search and rescue operations in heterogeneous terrain, when separate primary measurements obtained, for example, after reflections, could lead to a significant error. One possible way to improve the accuracy of positioning in such conditions is to use joint processing of TDOA and AOA primary measurements.

The problem of hybrid TDOA/AOA measurement processing to locate mobile station with stationary ground base stations on the plane was considered in [18] and demonstrated much higher location accuracy than TDOA only location, when the number of base stations is small and/or when the TDOA measurements have a relatively poor accuracy. Localization of radar emitters from a single sensor using multipath and TDOA-AOA measurements in a naval context was investigated in [19]. Results of [18] and [19] are valid for the 2D scenario, however localization in 3D is much more challenging than in 2D. Especially for AOA technique we are not able to apply the 2D AOA method to the azimuth and the elevation angle separately to obtain the source location, because two angles have to be used jointly in their respective non-linear measurement equations in order to determine the position of the source [20].

Problem of passive geolocation radiating emitter source in the three-dimensional (3D) space, using hybrid TDOA-AOA measurements was investigated in [21], however it considered the case of two stationary ground stations. Case of UAV based passive geolocation, using a hybrid TDOA-AOA was simulated in [22], however no performance evaluation due to inherent TDOA and AOA noise variation was done. Thus, the aim of current research is the development of mathematical model for positioning of radio emission sources with UAVs using TDOA-AOA measurement processing and performance evaluation investigation of hybrid measurement processing in handling TDOA and AOA noise for the case of UAV based passive geolocation.

The material in the paper is organized in the following order. Mathematical model for positioning with UAVs using TDOA-AOA measurement processing is presented in Section 2. Developed simulation model, scenario of geolocation and numerical results for performance of hybrid measurement processing in handling TDOA and AOA noise are given in Section 3. Finally, we draw conclusions in Section 4.

2. Mathematical model for positioning with UAVs using TDOA-AOA measurement processing

In this section we present following mathematical models, concerning positioning of radio emission sources with UAVs using TDOA-AOA measurement processing:

- UAV Based Passive Geolocation System Model;
- TDOA-AOA Error-Free Measurement Processing Model;
- Cramer-Rao Lower Bound for TDOA-AOA Measurement Processing Model;
- TDOA-AOA Noisy Measurement Processing Model.

2.1. UAV Based Passive Geolocation System Model

UAV based passive geolocation system under consideration, including flying segment based on transceiver stations aboard Unmanned Aerial Vehicles (UAVs) with terrestrial segment including stationary ground transceiver is shown in figure 1.

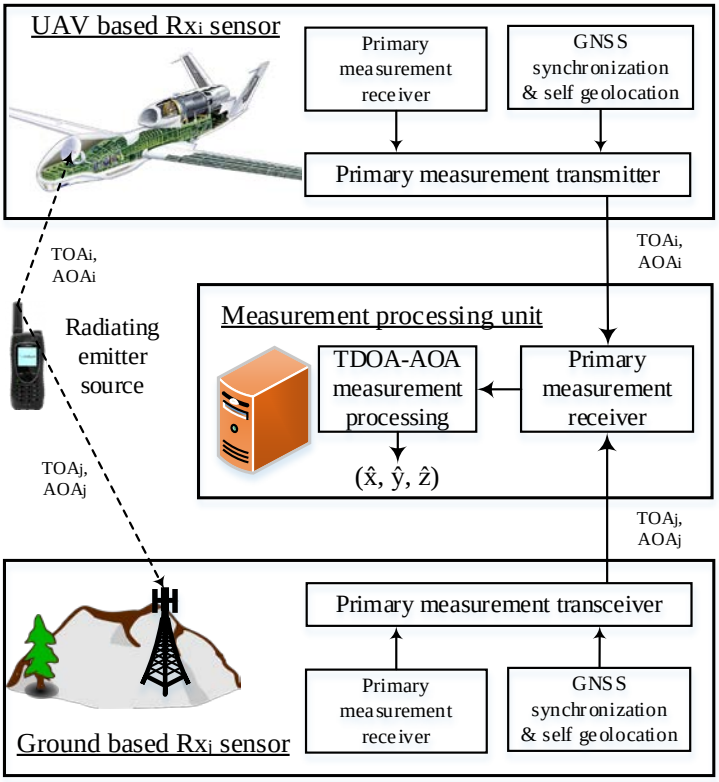

Figure 1. UAV based passive geolocation system.

Ground and UAV based passive receive sensors whose positions are available with Global Navigation Satellite Systems (GNSS) carry out the task of receiving primary Time of Arrival (TOA) and AOA measurements from packets transmitted by radiating emitter source. Single passive sensor can record the time stamp and direction of the received packet. Accurate time stamping is possible since each sensors has a GNSS receiver for time synchronization. Then, TOAs (timestamps) and AOAs of each sensor are forwarded to the measurement processing unit, which in turn using known sensor locations and hybrid TDOA-AOA measurement processing, estimate radiating emitter coordinates $\hat{\mathbf{x}}=(\hat{x},\hat{y},\hat{z})^{T}$.

If positioning is carried out by TDOA in three-dimensional space, at least four stationary receiving sensors are required to define three TDOA measurements from three pairs of sensors. Using of UAV

as moving sensor cooperatively with ground based sensor as a reference node, as shown in figure 2, allows to get multiple TDOA measurements along UAV flight path and hence reduce the number of required sensors to a pair.

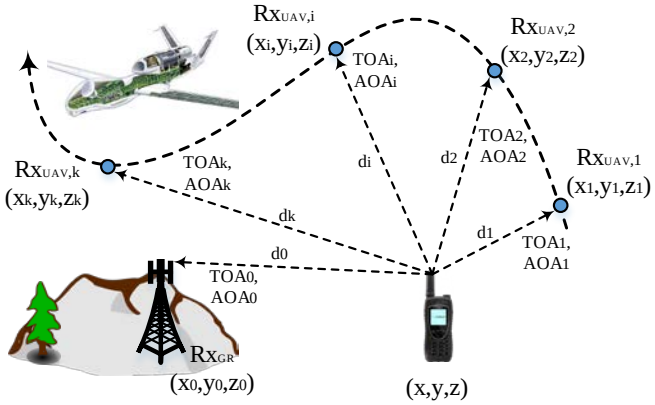

Figure 2. Using of UAV as moving sensor with ground based sensor.

2.2. TDOA-AOA Error-Free Measurement Processing Model

Let denote ground based receive sensor Rx_{GR} with available coordinates $\mathbf{x}_0=(x_0,y_0,z_0)^T$ as reference sensor and UAV based receive sensor Rx_{UAV} with available coordinates $\mathbf{x}_i=(x_i,y_i,z_i)^T$, where time intervals i=1…k correspond to synchronized timestamps, k – the number of primary measurements along UAV flight path. Let TOA_i be transmitted packet time of arrival for the signal radiating from the emitter, then TDOA between Rx_{UAV} and reference Rx_{GR} is defined by $t_{i,0}$ as

$$t_{i,0} = TOA_i - TOA_0 = d_{i,0}/c, \tag{1}$$

where c is speed of light and $d_{i,0}$ is range difference.

Actual error-free range difference is defined by

$$d_{i,0} = d_i - d_0, \tag{2}$$

where d_i is actual range between emitter with unknown coordinates $\mathbf{x}=(x,y,z)^T$ and sensor with available coordinates $\mathbf{x}_i=(x_i,y_i,z_i)^T$ defined as

$$d_i = \|\mathbf{x}-\mathbf{x}_i\|_2 = \sqrt{(x-x_i)^2+(y-y_i)^2+(z-z_i)^2}, \tag{3}$$

where $\|\cdot\|_2$ – norm operator over a vector in 3-D space [23].

Figure 3 shows TDOA-AOA geolocation geometry in the Cartesian coordinate system for the example time interval i. Emitter observation by two sensors results in one TDOA $t_{i,0}$ and two AOA pairs (θ_0,ϕ_0) and (θ_i,ϕ_i) of measurements.

As depicted in figure 3, projection of the range d_i between emitter and sensor on x-y plane is denoted by d_{ixy} and defined by

$$d_{ixy} = \sqrt{(x-x_i)^2+(y-y_i)^2}. \tag{4}$$

In matrix form error-free range difference measurement model $\mathbf{d}_0(\mathbf{x}) \in \mathbb{R}^{k\times 1}$ for i=1…k primary measurements along UAV flight path with reference receive sensor Rx_{GR} is defined by

$$\mathbf{d}_0(\mathbf{x}) = \begin{bmatrix} \sqrt{(x-x_1)^2+(y-y_1)^2+(z-z_1)^2} - \sqrt{(x-x_0)^2+(y-y_0)^2+(z-z_0)^2} \\ \sqrt{(x-x_2)^2+(y-y_2)^2+(z-z_2)^2} - \sqrt{(x-x_0)^2+(y-y_0)^2+(z-z_0)^2} \\ \vdots \\ \sqrt{(x-x_k)^2+(y-y_k)^2+(z-z_k)^2} - \sqrt{(x-x_0)^2+(y-y_0)^2+(z-z_0)^2} \end{bmatrix}. \tag{5}$$

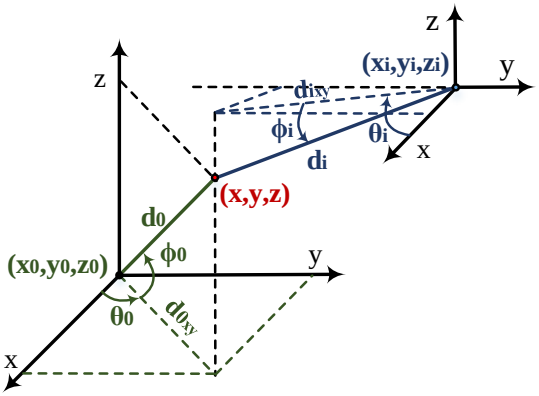

Figure 3. Geolocation geometry.

Actual error-free bearing pair b_i including azimuth θ_i and elevation ϕ_i AOAs from emitter with coordinates $\mathbf{x}=(x,y,z)^T$ to receive sensor with coordinates $\mathbf{x}_i=(x_i,y_i,z_i)^T$, i=1…k can be expressed as

$$b_i(\mathbf{x})=\begin{bmatrix}\theta_i\\ \phi_i\end{bmatrix}, \tag{6}$$

where

$$\theta_i=\operatorname{arctg}\left(\frac{y-y_i}{x-x_i}\right),$$

$$\phi_i=\operatorname{arctg}\left(\frac{z-z_i}{\sqrt{(x-x_i)^2+(y-y_i)^2}}\right). \tag{7}$$

For the sake of consistency in TDOAs and AOAs measurements, assume that emitter is stationary and bearing pair b_i is collected by ground based receive sensor Rx_{GR} for i=1…k time intervals along UAV flight path. Then in matrix form error-free bearing AOA measurement model $\mathbf{b}(\mathbf{x})\in\mathbb{R}^{2k\times 1}$ is

$$\mathbf{b}(\mathbf{x})=\begin{bmatrix}b_1(\mathbf{x})\\ b_2(\mathbf{x})\\ \vdots\\ b_k(\mathbf{x})\end{bmatrix}. \tag{8}$$

Actual error-free range difference (TDOA) and bearing (AOA) joint measurement model $f_i(\mathbf{x})$ for i^{th} time interval is defined as

$$f_i(\mathbf{x})=\begin{bmatrix}d_i(\mathbf{x})\\ b_i(\mathbf{x})\end{bmatrix}. \tag{9}$$

In matrix form range difference (TDOA) and bearing (AOA) joint measurement model $\mathbf{f}(\mathbf{x})\in\mathbb{R}^{3k\times 1}$ for i=1…k primary measurements along UAV flight path is defined by

$$\mathbf{f}(\mathbf{x})=\begin{bmatrix}\mathbf{d}(\mathbf{x})\\ \mathbf{b}(\mathbf{x})\end{bmatrix}. \tag{10}$$

2.3. Cramer-Rao Lower Bound for TDOA-AOA Measurement Processing Model

The CRLB gives a lower bound on variance attainable by any unbiased estimator using the same data, and thus it can be served as an important benchmark to compare with the root mean square error

(RMSE) of positioning algorithms [23]. The key in producing the CRLB is to construct the corresponding Fisher information matrix (FIM) **I**(**x**), computed at emitter location with coordinates $\mathbf{x}=(x,y,z)^T$. The diagonal elements of the FIM inverse are the minimum achievable variance values:

$$\mathrm{CRLB}(\mathbf{x}) = \mathrm{trace}\left(\mathbf{I}^{-1}(\mathbf{x})\right). \tag{11}$$

When the primary measurement errors are zero-mean Gaussian distributed, **I**(**x**) can be computed as [24]

$$\mathbf{I}(\mathbf{x}) = \left[\frac{\partial \mathbf{f}(\mathbf{x})}{\partial \mathbf{x}}\right]^{\mathrm{T}} \mathbf{C}^{-1} \left[\frac{\partial \mathbf{f}(\mathbf{x})}{\partial \mathbf{x}}\right], \tag{12}$$

where $\mathbf{C}$ denotes TDOA and AOA noise covariance matrix, and $\frac{\partial \mathbf{f}(\mathbf{x})}{\partial \mathbf{x}}$ is Jacobian matrix for joint measurement model $\mathbf{f}(\mathbf{x})$. Jacobian matrix $\frac{\partial \mathbf{d}_0(\mathbf{x})}{\partial \mathbf{x}} \in \mathbb{R}^{k\times 3}$ for $\mathbf{d}_0(\mathbf{x})$ is defined by

$$\frac{\partial \mathbf{d}_0(\mathbf{x})}{\partial \mathbf{x}} = \begin{bmatrix} \frac{x-x_1}{d_1} - \frac{x-x_0}{d_0} & \frac{y-y_1}{d_1} - \frac{y-y_0}{d_0} & \frac{z-z_1}{d_1} - \frac{z-z_0}{d_0} \\ \frac{x-x_2}{d_2} - \frac{x-x_0}{d_0} & \frac{y-y_2}{d_2} - \frac{y-y_0}{d_0} & \frac{z-z_2}{d_2} - \frac{z-z_0}{d_0} \\ \vdots & \vdots & \vdots \\ \frac{x-x_k}{d_k} - \frac{x-x_0}{d_0} & \frac{y-y_k}{d_k} - \frac{y-y_0}{d_0} & \frac{z-z_k}{d_k} - \frac{z-z_0}{d_0} \end{bmatrix}, \tag{13}$$

where d_i is computed according to (3). Jacobian matrix $\frac{\partial \mathbf{b}(\mathbf{x})}{\partial \mathbf{x}} \in \mathbb{R}^{2k\times 3}$ for $\mathbf{d}_0(\mathbf{x})$ is defined by

$$\frac{\partial \mathbf{b}(\mathbf{x})}{\partial \mathbf{x}} = \begin{bmatrix} -\frac{(y-y_1)}{d_{1xy}^2} & \frac{(x-x_1)}{d_{1xy}^2} & 0 \\ -\frac{(x-x_1)(z-z_1)}{d_1^2 d_{1xy}} & -\frac{(y-y_i)(z-z_i)}{d_1^2 d_{1xy}} & \frac{d_{1xy}}{d_1^2} \\ \vdots & \vdots & \vdots \\ -\frac{(y-y_k)}{d_{kxy}^2} & \frac{(x-x_k)}{d_{kxy}^2} & 0 \\ -\frac{(x-x_k)(z-z_k)}{d_k^2 d_{kxy}} & -\frac{(y-y_k)(z-z_k)}{d_k^2 d_{kxy}} & \frac{d_{kxy}}{d_k^2} \end{bmatrix}, \tag{14}$$

where d_i and d_{ixy} defined according to (3) and (4) respectively.

Jacobian matrix for joint measurement model $\mathbf{f}(\mathbf{x})$ is defined from (13) and (14) by

$$\frac{\partial \mathbf{f}(\mathbf{x})}{\partial \mathbf{x}} = \begin{bmatrix} \frac{\partial \mathbf{d}_0(\mathbf{x})}{\partial \mathbf{x}} \\ \frac{\partial \mathbf{b}(\mathbf{x})}{\partial \mathbf{x}} \end{bmatrix}. \tag{15}$$

2.4. TDOA-AOA Noisy Measurement Processing Model

Expressions (2) and (6) represent error-free values of TDOA and AOA, however in practice noise is always present in measurements. Noisy TDOA can be rewritten from (2) as

$$d_{i,0} = d_i - d_0 + n_{di} \tag{16}$$

where n_{di} is measurement noise for $d_{i,0}$ with TDOA standard deviation σ_{TDOA}. Employing technique, proposed in [24], under the assumption that ground based receive sensor Rx_{GR} is in the Cartesian coordinate system origin, we can represent TDOA measurement processing model in matrix form as [22]

$$\mathbf{m}_{TDOA} = \mathbf{g}_{TDOA}\mathbf{X} + \mathbf{n}_{TDOA} \tag{17}$$

where

$$\mathbf{m}_{TDOA} = \frac{1}{2}\begin{bmatrix} d_{1,0}^2 - K_1 \\ d_{2,0}^2 - K_2 \\ \vdots \\ d_{k,0}^2 - K_k \end{bmatrix}, \mathbf{g}_{TDOA} = \begin{bmatrix} -x_1 & -y_1 & -z_1 & -d_{1,0} \\ -x_2 & -y_2 & -z_2 & -d_{2,0} \\ \vdots & \vdots & \vdots & \vdots \\ -x_k & -y_k & -z_k & -d_{k,0} \end{bmatrix},$$
$$\mathbf{n}_{TDOA} = \left[n_{d1}, n_{d2}, \ldots, n_{dk}\right]^T, K_i = x_i^2 + y_i^2 + z_i^2, \tag{18}$$

and $\mathbf{X} = \left[x, y, z, d_0\right]^T$ is the vector of unknown variables.

Noisy AOA was also considered in [22], however only ground based sensor measured AOA. Consider the case of stationary emitter, illustrated in figure 3, where Rx_{GR} measures single AOA pair (θ_0,ϕ_0) and Rx_{UAV} measures k AOA pairs (θ_i,ϕ_i), i=1…k along UAV flight path. Then we can represent AOA measurement processing model in matrix form as [22]

$$\mathbf{m}_{AOA} = \mathbf{g}_{AOA}\mathbf{X} + \mathbf{n}_{AOA}, \tag{19}$$

where

$$\mathbf{m}_{AOA} = \begin{bmatrix} 0 \\ 0 \\ \vdots \\ 0 \\ 0 \end{bmatrix}, \mathbf{g}_{AOA} = \begin{bmatrix} -\sin\theta_0 & \cos\theta_0 & 0 & 0 \\ -\sin\phi_0/\cos\theta_0 & 0 & \cos\phi_0 & 0 \\ \vdots & \vdots & \vdots & \vdots \\ -\sin\theta_k & \cos\theta_k & 0 & 0 \\ -\sin\phi_k/\cos\theta_k & 0 & \cos\phi_k & 0 \end{bmatrix},$$
$$\mathbf{n}_{AOA} = \left[d_{0xy}n_{\theta_0}, d_0 n_{\phi_0}, \ldots, d_{ixy}n_{\theta_i}, d_i n_{\phi_i}\right]^T, \tag{20}$$

where $\left(n_{\theta i}, n_{\phi i}\right)$ is measurement noise for (θ_i,ϕ_i), i=0…k, with AOA standard deviation σ_{AOA}.

Joint processing of TDOA and AOA primary measurements by combining (17) and (19) gives a set of overdetermined location equations

$$\begin{bmatrix} \mathbf{m}_{TDOA} \\ \mathbf{m}_{AOA} \end{bmatrix} = \begin{bmatrix} \mathbf{g}_{TDOA} \\ \mathbf{g}_{AOA} \end{bmatrix}\mathbf{X} + \begin{bmatrix} \mathbf{n}_{TDOA} \\ \mathbf{n}_{AOA} \end{bmatrix} \tag{21}$$

3. Simulation model

Simulation scenario described further is based on the assumption of ideal synchronization between sensors of the terrestrial and flying segments aboard UAV. Simulation model was realized in MatLab and included arrangement, estimation and visualization subsystems [25]–[29].

Positioning of the emitter was performed for scenario when it is located in three-dimensional space at the point (5, 4.3, 1.5) km in an area with a size of (10 km × 10 km × 5 km) as depicted in figure 4 [26]. UAV flies circumferentially over the working area at a constant altitude z = 4 km [26]. Choice of circle trajectory of the UAV movement for simulation is due to the fact it is the most frequently encountered for analyzing when positioning using the flying segment [29].

A set of overdetermined location equations was solved with Levenberg-Marquardt (LM) positioning algorithm [30] and compared with Cramer-Rao lower bound (CRLB) [21].

The root-mean-square error (RMSE) of coordinates estimate of the emitter source is [31].

$$\text{RMSE}=\sqrt{\text{E}\left\{\sqrt{\left(x-\hat{x}\right)^2+\left(y-\hat{y}\right)^2+\left(z-\hat{z}\right)^2}\right\}} \tag{22}$$

wher $\hat{\mathbf{x}}=\left[\hat{x},\hat{y},\hat{z}\right]$ is emitter LM location estimate.

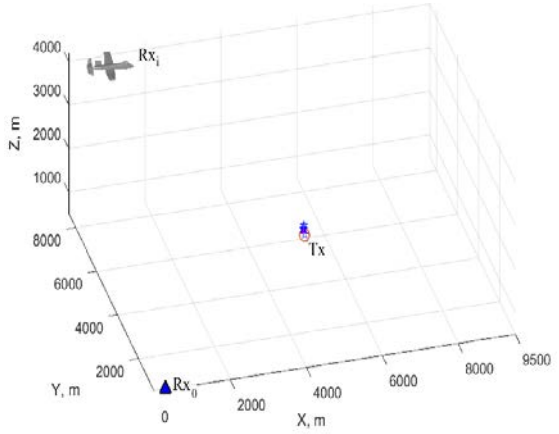

Figure 4. Simulation scenario.

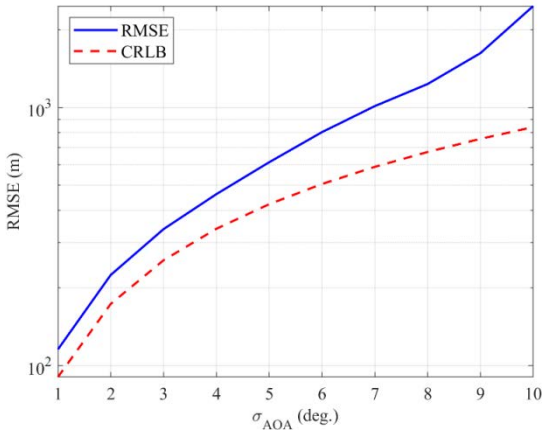

Figure 5. Emitter RMSE versus σ_{AOA}.

Previous simulation results with six sensors and TDOA only measurement processing achieved RMSE of approximately 10 m [25]–[29]. Figure 5 shows a performance of hybrid TDOA-AOA measurement processing location estimation in terms of RMSE versus the AOA standard deviation σ_{AOA} computed during simulation when TDOA standard deviation σ_{TDOA} is fixed at 10 m.
It can be seen from figure 5, that positioning performance with only two sensors is rather coarse comparing to the case of six sensors even with accurate primary AOA measurements acquisition.

4. Conclusion

In this paper we evaluated the positioning accuracy of hybrid TDOA-AOA measurement processing location estimation with handling TDOA and AOA noise. Simulation results in terms of RMSE versus the AOA standard deviation σ_{AOA} demonstrated that positioning performance with only two sensors is rather coarse comparing to the case of six sensors even with accurate primary AOA measurements acquisition.

5. References

[1] Hayat, S. Survey on Unmanned Aerial Vehicle Networks for Civil Applications: A Communications Viewpoint / S. Hayat, E. Yanmaz, R. Muzaffar // IEEE Communications Surveys & Tutorials. – 2016. – Vol. 18(4). – P. 2624-2661.

[2] Saputra, O.D. UAV-based localization for distributed tactical wireless networks using archimedean spiral / O.D. Saputra, M. Irfan, N.N. Putri, S.Y. Shin // International Symposium on Intelligent Signal Processing and Communication Systems (ISPACS). – Nusa Dua, 2015. – P. 392-396.

[3] Kim, D. UAV-Based Localization Scheme for Battlefield Environments / D. Kim, K. Lee, M. Park, J. Lim // IEEE Military Communications Conference (MILCOM). – San Diego, CA, 2013. – P. 562-567.

[4] Stamatescu, G. Cognitive radio as solution for ground-aerial surveillance through WSN and UAV infrastructure / G. Stamatescu, D. Popescu, R. Dobrescu // Proceedings of the 6th International Conference on Electronics. – Computers and Artificial Intelligence (ECAI). – Bucharest, 2014. – P. 51-56.

[5] Santana, G.M.D. Cognitive Radio for UAV communications: Opportunities and future challenges / G.M.D. Santana, R.S. Cristo, C. Dezan, J. Diguet, D.P.M. Osorio, K.R.L.J.C. Branco // International Conference on Unmanned Aircraft Systems (ICUAS), Dallas, 2018. – P. 760-768.

[6] Waharte, S. Supporting Search and Rescue Operations with UAVs / S. Waharte, N. Trigoni // International Conference on Emerging Security Technologies. – Canterbury, 2010. – P. 142-147.

[7] Torrieri, D.J. Statistical Theory of Passive Location Systems / D.J. Torrieri // IEEE Transactions on Aerospace and Electronic Systems. – 1984. – Vol. AES-20(2). – P. 183-198.
[8] Du, H.-J. Passive Geolocation Using TDOA Method from UAVs and Ship/Land-Based Platforms for Maritime and Littoral Area Surveillance / H.-J. Du, P.Y. Lee. – Ottawa, Canada: Technical Memorandum, 2004. – 38 p.
[9] Fletcher, F. Recursive estimation of emitter location using TDOA measurements from two UAVs / F. Fletcher, B. Ristic, D. Musicki // 10th International Conference on Information Fusion. – Quebec, 2007. – P. 1-8.
[10] Okello, N. Comparison of Recursive Algorithms for Emitter Localisation using TDOA Measurements from a Pair of UAVs / N. Okello, F. Fletcher, D. Musicki, B. Ristic // IEEE Transactions on Aerospace and Electronic Systems. – 2011. – Vol. 47(3). – P. 1723-1732.
[11] Musicki, D. Mobile Emitter Geolocation and Tracking Using TDOA and FDOA Measurements / D. Musicki, R. Kaune, W. Koch // IEEE Transactions on Signal Processing. – 2010. – Vol. 58(3). – P. 1863-1874.
[12] Wang, Z. A low-cost, near-real-time two-UAS-based UWB emitter monitoring system / Z. Wang, E. Blasch, G. Chen, D. Shen, X. Lin, K. Pham // IEEE Aerospace and Electronic Systems Magazine. – 2015. – Vol. 30(11). – P. 4-11.
[13] Bamberger, J.R. Autonomous geo location of rf emitters using small, unmanned platforms / R.J. Bamberger, J.G. Moore, R.P. Goonasekeram, D.H. Scheidt // Johns Hopkins APL Technical Digest. – 2013. – Vol. 32(3). – P. 636-646.
[14] Magers, M.A. Geolocation of RF Emitters Using a Low-Cost UAV-Based Approach / M.A. Magers // M. Sci. thesis, Air Force Institute of Technology. – Write-Patterson Air Force Base, Ohio, United States, 2016. – 113 p.
[15] Hasanzade, M. Localization and tracking of RF emitting targets with multiple unmanned aerial vehicles in large scale environments with uncertain transmitter power / M. Hasanzade, O. Herekoglu, N.K. Ure, E. Koyuncu, R. Yeniceri, G. Inalhan // International Conference on Unmanned Aircraft Systems (ICUAS). – Miami, FL, USA, 2017. – P. 1058-1065.
[16] Dehghan, S.M.M. Optimal path planning for DRSSI based localization of an RF source by multiple UAVs / S.M.M. Dehghan, H. Moradi, S.A.A. Shahidian // Second RSI/ISM International Conference on Robotics and Mechatronics. – Tehran, 2014. – P. 558-563.
[17] Koohifar, F. Autonomous Tracking of Intermittent RF Source Using a UAV Swarm / F. Koohifar, I. Guvenc, M.L. Sichitiu // IEEE Access. – 2018. – Vol. 6. – P. 15884-15897.
[18] Cong, L. Hybrid TDOA/AOA mobile user location for wideband CDMA cellular systems / L. Cong, W. Zhuang // IEEE Trans. Wireless Commun. – 2002. – Vol. 1. – P. 439-447.
[19] Giacometti, R. Localization of radar emitters from a single sensor using multipath and TDOA-AOA measurements in a naval context / R. Giacometti, A. Baussard, D. Jahan, C. Cornu, A. Khenchaf, J. Quellec // 24th European Signal Processing Conference (EUSIPCO). – Budapest, 2016. – P. 692-696.
[20] Wang, Y. An Asymptotically Efficient Estimator in Closed-Form for 3-D AOA Localization Using a Sensor Network / Y. Wang, K.C. Ho // IEEE Transactions on Wireless Communications. – 2015. – Vol. 14(12). – P. 6524-6535.
[21] Yin, J. A Simple and Accurate TDOA-AOA Localization Method Using Two Stations / J. Yin, Q. Wan, S. Yang, K.C. Ho // IEEE Signal Processing Letters. – 2016. – Vol. 23(1). – P. 144-148.
[22] Du H.-J. Simulation of multi-platform geolocation using a hybrid TDOA-AOA method / H.-J. Du, P.Y. Lee // Ottawa, Canada: Technical Memorandum, 2004. – 44 p.
[23] Zekavat, R. Handbook of position location: Theory practice and advances / R. Zekavat, R.M. Buehrer // John Wiley & Sons, 2011. – 1255 p.
[24] Chan, Y.T. A simple and efficient estimator for hyperbolic location / Y.T. Chan, K.C. Ho // IEEE Trans. Signal Process. – 1994. – Vol. 42. – P. 1905-1915.
[25] Al-Odhari, A.H.A. Positioning of the radio source based on time difference of arrival method using unmanned aerial vehicles / A.H.A. Al-Odhari, G. Fokin, A. Kireev // Systems of Signals

Generating and Processing in the Field of on Board Communications. – Moscow, 2018. – P. 1-5.
[26] Fokin, G. Algorithm for Positioning in Non-line-of-Sight Conditions Using Unmanned Aerial Vehicles / G. Fokin, A.A.H. Ali // Lecture Notes in Computer Science. – 2018. – Vol. 11118. – P. 496-508.
[27] Fokin, G.A. Positioning of the moving radiation source using Time Difference of Arrival method / G.A. Fokin, A.H. Alodhari // T-Comm (Media Publisher). – 2017. – Vol. 11(4). – P. 41-46.
[28] Fokin, G.A. TDOA measurement processing for positioning using unmanned aerial vehicles / G.A. Fokin, A.H. Alodhari // T-Comm (Media Publisher). – 2018. – Vol. 12(7). – P. 52-58.
[29] Al-Odhari, A. Positioning of Radio Emission Sources in Hilly Terrain Using Unmanned Aerial Vehicles / A. Al-Odhari, G. Fokin // Proceedings of Telecommunication Universities. – 2018. – Vol. 4(2). – P. 5-17.
[30] Sivers, M. LTE Positioning Accuracy Performance Evaluation / M. Sivers, G. Fokin // Lecture Notes in Computer Science. – 2015. – Vol. 9247. – P. 393-406.
[31] Mashkov, G. Experimental validation of multipoint joint processing of range measurements via software-defined radio testbed / G. Mashkov, E. Borisov, G. Fokin // 18th International Conference on Advanced Communication Technology (ICACT). – Pyeongchang, 2016. – P. 268-273.
[32] Petrov, A.A. Some Directions of Quantum Frequency Standard Modernization for Telecommunication Systems / A.A. Petrov, V.V. Davydov, N.M. Grebenikova // Lecture Notes in Computer Science (including subseries Lecture Notes in Artificial Intelligence and Lecture Notes in Bioinformatics). – 2018. – Vol. 11118. – P. 641-648.
[33] Petrov, A.A. Features of magnetic field stabilization in caesium atomic clock for satellite navigation system / A.A. Petrov, N.M. Grebenikova, N.A. Lukashev, N.V. Ivanova, N.S. Rodygina, A.V. Moroz // Journal of Physics: Conference Series. – 2018. – Vol. 1038(1). – P. 012032.
[34] Podstrigaev, A.S. Features of the Development of Transceivers for Information and Communication Systems Considering the Distribution of Radar Operating Frequencies in the Frequency Range / A.S. Podstrigaev, A.V. Smolyakov, V.V. Davydov, N.S. Myazin, M.G. Slobodyan // Lecture Notes in Computer Science (including subseries Lecture Notes in Artificial Intelligence and Lecture Notes in Bioinformatics). – 2018. – Vol. 11118. – P. 509-515.

Acknowledgments
This work was supported by the Ministry of Science and Education of the Russian Federation with Grant of the President of the Russian Federation for the state support of young Russian scientists № МК-3468.2018.9.